haematologica
Journal of the Ferrata Storti Foundation

CXCR2 deficiency with myelokathexis caused by a novel variant: correction via CRISPR/Cas9

by Daniëla M. Hinke, Sofie R. Dorset, Eirik Bratland, Jonas H. Wolff, Astrid M. Olsnes, Jacob Giehm Mikkelsen, Lars O. Helgeland, Rasmus O. Bak, Andreas Benneche and Trine H. Mogensen

Received: May 7, 2025.
Accepted: August 19, 2025.

Citation: Daniëla M. Hinke, Sofie R. Dorset, Eirik Bratland, Jonas H. Wolff, Astrid M. Olsnes, Jacob Giehm Mikkelsen, Lars O. Helgeland, Rasmus O. Bak, Andreas Benneche and Trine H. Mogensen. CXCR2 deficiency with myelokathexis caused by a novel variant: correction via CRISPR/Cas9. Haematologica. 2025 Aug 28. doi: 10.3324/haematol.2025.288111 [Epub ahead of print]

CXCR2 deficiency with myelokathexis caused by a novel variant: correction via CRISPR/Cas9

Daniëla M. Hinke[1,2,3], Sofie R. Dorset[1], Eirik Bratland[4], Jonas H. Wolff[1,3], Astrid M. Olsnes[5,6], Jacob Giehm Mikkelsen[1,3], Lars Helgeland[7], Rasmus O. Bak[1], Andreas Benneche[4], and Trine H. Mogensen[1,2,3]*

1. Department of Biomedicine, Aarhus University, Aarhus, Denmark

2. Department of Infectious Diseases, Aarhus University Hospital, Aarhus, Denmark

3. Center for Immunology of Viral infections (CIVIA), Aarhus University, Aarhus, Denmark

4. Department of Medical Genetics, Haukeland University Hospital, Bergen, Norway

5. Department of Clinical Science, University of Bergen, Norway

6. Department of Hematology, Department of medicine, Haukeland University Hospital, Bergen, Norway

7. Department of Pathology, Haukeland University Hospital, Bergen, Norway

Running head: Gene editing for a new variant in CXCR2 deficiency

***Corresponding author:** Trine H Mogensen, Department of Biomedicine, Aarhus University, Wilhelm Meyers Allé 4, 8000 Aarhus C, Denmark; mail: Trine.mogensen@biomed.au.dk

Author contributions

THM and AB conceived the idea and discussed the patient clinical history and genetic and immunological evaluation. AB and EB performed genetic analysis and identified and described the CXCR2 variant; EB performed structural analysis of the CXCR2 variant and contributed with molecular and structural biology input; LH did the histopathology of the bone marrow and described and quantified the myelokathexis. ROB and SRD designed the CRISPR strategy; DMH, SRD, and JHW performed experiments and analyzed the data together with THM, ROB, and JGM. AMO and THM cared for the patients. THM, AB, and DMH wrote the first draft of the manuscript, and all authors read, corrected and approved the final version of the manuscript.

Conflicts of interest: The authors have no COIs to disclose

Data sharing: Original data and protocols are available upon request from the corresponding author.

Acknowledgements
We warmly thank the family for participating in the study. In addition, we thank technician Bettina Bundgaard for excellent technical assistance. Flow cytometry was performed at the FACS Core Facility, Aarhus University, Denmark. Confocal imaging was performed at the Bioimaging Core Facility, Health, Aarhus University, Denmark.

Funding
THM is supported by the Independent Research Fund Denmark (0134-00006B), the Novo Nordisk Foundation (NNF21OC0067157; NNF20OC0064890), the Lundbeck Foundation (R268-2016-3927), The innovation Fund Denmark (PASCAL-MID, 8056-00010B), the HORIZON-HLTH-2021-DISEASE-04 program under grant agreement 101057100 (UNDINE), the Danish National Research Foundation under the grant agreement DNRF164 (CiViA). DMH received funding from Innovation Fund Denmark (PASCAL-MID, 8056-00010B), and the HORIZON-HLTH-2021-DISEASE-04 program under grant agreement 101057100 (UNDINE). ROB and JGM received funding from Innovation Fund Denmark (PASCAL-MID, 8056-00010B). DMH was supported by AP Møller Foundation for the Advancement of Medical research (2024-00880) and the Aase and Ejnar Danielsens Fund for Medical Research (24-10-0515).

Myelokathexis is a severe form of neutropenia caused by retention of neutrophils in the bone marrow, with accumulation of both live and apoptotic neutrophils, resulting in neutropenia in peripheral blood(1, 2). One cause of myelokathexis is WHIM syndrome, a rare inborn error of immunity (IEI) named after its characteristics, including HPV-induced Warts, Hypogammaglobulinemia, recurrent Infections and Myelokathexis(3, 4). More recently biallelic loss-of-function variants in *CXCR2* was reported to represent another WHIM-like IEI with neutropenia and varying degrees of myelokathexis(5-7). CXCR2 deficiency is exceedingly rare with currently nine cases published(5-7). The neutropenia characteristic of WHIM syndrome and CXCR2 deficiency stems from the essential roles of CXCR4 and CXCR2 in inhibiting and promoting neutrophil egress from the bone marrow into the blood stream, respectively. Stimulation of CXCR4 by its ligand C-X-C motif ligand 12 (CXCL12), which is constitutively expressed by bone marrow stromal cells, promotes neutrophil retention, whereas CXCR2 stimulation by interleukin 8 (IL-8) promotes release of neutrophils from the bone marrow to peripheral blood(8, 9). CXCR2, also known as IL-8 receptor β, is a G-protein-coupled seven transmembrane receptor for the CXC subclass of chemokines(10) expressed predominantly on neutrophils, and to a lesser extent on monocytes, macrophages, NK cells, and endothelial cells(11, 12).

Two brothers from a family of healthy non-consanguineous Norwegian parents and one healthy brother presented with severe neutropenia. Patient 1 (P1) had been suffering from frequent upper respiratory tract infections since the age of one. He was diagnosed with neutropenia at three years of age at which time a bone marrow biopsy showed high cellularity (80% of cells being granulocytes) and myelokathexis. Immunophenotyping of blood PBMCs showed normal distribution of T, B, and NK cells with marginally increased fraction of plasmablasts. At age 29, he still experiences frequent tonsillitis/pharyngitis and suffers from severe gingival ulcerations. His neutrophil count has continuously been decreased in the range of 0.5-1.2 x 10^9/L [normal range 1.8 - 6.9x10^9/L] **(Figure 1A, Supplementary Figure 1A and B)**. P2, the younger brother of P1, was admitted to hospital with pneumonia at the age of three years and was diagnosed with neutropenia at the age of 16, at which time hematological evaluation revealed persistent neutropenia. A

bone marrow biopsy showed increased myelopoiesis and myelokathexis (estimated to affect ~33% mature granulocytes), with normal maturation of neutrophils, reminiscent of previous descriptions of myelokathexis in conjunction with WHIM syndrome **(Figure 1B)**. During follow up, the patient's neutrophil count has repeatedly been in the range of 0.1-0.2x10^9/L **(Supplementary Figure 1C)**. At age 23 his major symptoms are ulcerations in the nose and oral cavity. Both parents and a third younger brother were healthy without oral ulcerations or infections (although the mother experienced one episode of neutropenia) and with neutrophil counts in the lower normal range (father 2.1x10^9/L, mother 2.8x10^9/L and brother 3.2x10^9/L). The patients, their family, and healthy controls were included following oral and written consent in accordance with The Helsinki Declaration and national ethics guidelines. The study was approved by the Danish National Committee on Health Ethics, the Data Protection Agency, and Institutional Review Board.

Due to the notable presentation of the two brothers with isolated severe neutropenia and myelokathexis combined with the family pedigree, an autosomal recessive IEI with neutropenia was suspected. Genetic analysis by whole exome sequencing (WES) revealed that P2 was homozygous for a *CXCR2* missense variant c.865C>T, resulting in substitution of a positively charged arginine to neutral cysteine amino acid (p.R289C) **(Figure 1C).** P1 was found to be homozygous for the same variant by Sanger sequencing, whereas both parents and the third brother were heterozygous carriers of the variant **(Figure 1D; Supplementary Fig. 1D).** The variant was classified as likely pathogenic according to the American College of Medical Genetics and Genomics (ACMG)/Association for Molecular Pathology (AMP) sequence variant guidance(13), (For details see **Supplementary Figure 1E**). The CXCR2 R289C missense variant is rare, has a relatively high combined annotation dependent depletion (CADD) score of 23.5 and shows a high degree of evolutionary conservation **(Figure 1C and E)**. No individuals homozygous for the specific CXCR2 c.865C>T variant have been reported in GnomAD v.4.1.0(5-7), whereas heterozygosity for this variant has been associated with reduced neutrophil counts(5). According to protein structure analysis(14) CXCR2 Arg289 is located towards the extracellular end of the seventh transmembrane alpha helix **(Figure 1F)**.

To investigate the deleteriousness of patient CXCR2 patient variant, we used HeLa cells as a model. Transfected HeLa cells expressing either CXCR2 WT or R289C showed that the patient variant led to reduced CXCR2 protein expression in the cytosol as well as at the cell surface **(Figure 2A-B)**. Furthermore, the CXCR2 R289C variant failed to mediate phosphorylation of the MAPK signaling kinase Erk1/2 in response to IL-8 stimulation, revealing impaired signaling **(Figure 2C-D)**. Treating transfected HeLa cells with the proteasome inhibitor MG-132 selectively increased the abundance of CXCR2 R289C protein and not CXCR2 WT **(Figure 2E-F)**, suggesting that CXCR2 R289C undergoes accelerated degradation by the proteasome pathway, thereby accounting for the reduced levels of CXCR2 variant expression. Next, we performed confocal microscopy to visualize CXCR2 in relation to the ER and Golgi in transfected HeLa cells. While CXCR2 WT was expressed at high levels and with even distribution on the cell surface, the CXCR2 R289C variant was largely undetectable at the cell surface but localized intracellularly in a perinuclear distribution. Furthermore, we observed that a significantly increased fraction of CXCR2 R289C was colocalized with both the ER and Golgi apparatus when compared to CXCR2 WT protein **(Figure 2G-J, Supplementary Figure 2A-B)**. These data suggest a posttranscriptional defect impairing synthesis and trafficking of the CXCR2 R289C variant through the secretory pathway, ultimately abolishing the expression of a functional CXCR2 receptor protein at the cell surface.

Having established the impaired function of the CXCR2 R289C variant we examined patient blood cells. In patient PBMCs, expression of *CXCR2* mRNA was comparable to healthy controls, whereas levels of CXCR2 protein were reduced **(Figure 3A-C)**. Flow cytometry demonstrated that CXCR2 surface expression was significantly reduced on patient NK cells, monocytes, and neutrophils compared to controls **(Figure 3D-G, Supplementary Figure 2C-D).** A trans-well migration assay using whole blood revealed markedly reduced ability of patient neutrophils to migrate towards IL-8 **(Figure 3H)**. Finally, to explore the therapeutic potential of gene correction, we used CRISPR/Cas9 gene editing with DNA templates for homology directed repair (HDR) to correct the deleterious *CXCR2* gene variant in patient PBMCs. We expanded T cells from patient PBMCs and performed gene editing on these cells **(Figure 3I).** This led to almost 100% editing

efficiency for correction of the *CXCR2* c.865C>T gene variant in patient cells **(Figure 3J)**. CRISPR activation (CRISPR)a was used to induce CXCR2 transcription which resulted in similarly increased levels of CXCR2 surface expression in gene-edited patient and healthy control T cells **(Figure 3K-L, Supplementary Figure 2E)**. These results confirm that the CXCR2 defect caused by the R289C variant can be corrected via gene editing to reconstitute expression of CXCR2 WT. Importantly, these data demonstrate the feasibility of this editing approach and imply a therapeutic potential for CRISPR/Cas9 gene editing for the two patients with CXCR2 deficiency, and in general for patients with this condition.

The clinical presentation of these patients with a novel CXCR2 R289C missense variant, including isolated neutropenia and myelokathexis with moderate susceptibility to infection, are largely in line with the previously published cases on CXCR2 deficiency(5-7). Although we initially hypothesized that the CXCR2 R289C variant might interrupt IL-8 binding to the CXCR2 receptor, we instead established the mechanism to be failure of the variant to be expressed at the cell surface, likely accounting for the defective signaling and impaired chemotaxis of patient cells. At the molecular level this may be due to improper protein folding in the ER and impaired trafficking through the secretory pathway to the cell surface, combined with increased protein turnover via proteasomal degradation in the cytosol. In contrast to our findings of reduced CXCR2 surface expression on neutrophils, monocytes and NK cells, Marin-Esteban et al. presented a case in which the R289C variant in heterozygosity did not lead to a reduced CXCR2 surface expression, suggesting that homozygosity is required for this variant to result in loss of surface expression.

CXCR2 deficiency was first described by Auer et al. reporting on a homozygous variant in two siblings (CXCR2 c.968del/p.His323LeufsTer7) who suffered from congenital myelokathexis and neutropenia with recurrent bacterial infections(5). Another publication reported four patients with different *CXCR2* variants, including a homozygous deletion on chromosome 2q35 affecting the entire *CXCR2* locus, homozygous missense variants (p.Arg144Cys and p.Ala212Trp) and compound heterozygosity for the nonsense variant p.Arg184Ter and the variant we describe herein (p.Arg289Cys)(6) **(Supplementary table 1)**. All four had

severe oral lesions, and two responded well to G-CSF-treatment, but only the patient carrying the whole-gene deletion had myelokathexis, underscoring the variability of CXCR2 deficiency severity(6). Finally, three additional families with CXCR2 deficiency were recently described(7). The missense variant pArg144His was present in all three families, either in homozygous or compound heterozygous combination. In cases where bone marrow investigation was performed, a hypercellular myeloid series but no overt myelokathexis was described. The clinical phenotype was characterized by recurrent upper airway and skin infections together with oral ulcerations. Overall, the currently published cases of CXCR2 deficiency reveal some variability regarding the degree of neutropenia, the extent of myelokathexis, abnormalities in IgG, IgM, and/or IgA levels, and the severity of the infectious phenotype. Indeed, myelokathexis is a rare feature among individuals with CXCR2 deficiency and was reported in only two out of nine published cases, of which one was only partial (35%)(5-7) **(Supplementary table 1)**. Collectively, neutropenia and oral ulcerations are key features and common characteristics of CXCR2 deficiency, prompting the suggestion that CXCR2 deficiency be regarded as a genetic etiology of severe neutropenia that may or may not be associated with myelokathexis and thus distinct from WHIM syndrome. Moreover, our results together with other reports suggest CXCR2 R289C heterozygosity as a potential risk factor for neutropenia. Whether patients with CXCR2 deficiency may experience an increased risk of malignancy, like the case for WHIM syndrome, remains undetermined.

Treatment options for WHIM syndrome and CXCR2 deficiency are limited. G-CSF is commonly used to treat neutropenia since it drives neutrophil differentiation and neutrophil mobilization(15). Another treatment approach consists of the CXCR4 antagonists plerixafor(16) and mavorixafor(17), which block CXCL12-binding to CXCR4 and thereby counteract the inhibition of neutrophil efflux from the bone marrow. Finally, we here demonstrate efficient HDR CRISPR/Cas correction of CXCR2 in patient PBMCs, suggesting that a similar strategy in patient CD34+ hematopoietic stem cells may constitute a curative gene therapy for these patients following further validation of efficiency and safety. To our knowledge this is the first in vitro attempt at demonstrating CRISPR/Cas gene correction in CXCR2 deficiency.

References

1. Zuelzer WW, Evans RK, Goodman J. Myelokathexis - A New Form of Chronic Granulocytopenia. N Engl J Med. 1964;270(14):699-704.
2. Krill Carl E, Smith Hugo D, Mauer Alvin M. Chronic Idiopathic Granulocytopenia. N Engl J Med. 1964;270(19):973-979.
3. Wetzler M, Talpaz M, Kleinerman ES, et al. A new familial immunodeficiency disorder characterized by severe neutropenia, a defective marrow release mechanism, and hypogammaglobulinemia. Am J Med. 1990;89(5):663-672.
4. Heusinkveld LE, Majumdar S, Gao JL, McDermott DH, Murphy PM. WHIM Syndrome: from Pathogenesis Towards Personalized Medicine and Cure. J Clin Immunol. 2019;39(6):532-556.
5. Auer PL, Teumer A, Schick U, et al. Rare and low-frequency coding variants in CXCR2 and other genes are associated with hematological traits. Nat Genet. 2014;46(6):629-634.
6. Marin-Esteban V, Youn J, Beaupain B, et al. Biallelic CXCR2 loss-of-function mutations define a distinct congenital neutropenia entity. Haematologica. 2021;107(3):765-769.
7. Klimiankou M, Tesakov I, Tsaknakis G, et al. Expanding the genetic landscape of congenital neutropenia: CXCR2 mutations in three families revealed through whole exome sequencing. Haematologica. 2024;109(12):4140-4144.
8. Burdon PCE, Martin C, Rankin SM. Migration across the sinusoidal endothelium regulates neutrophil mobilization in response to ELR + CXC chemokines. Br J Haematol. 2008;142(1):100-108.
9. Eash KJ, Greenbaum AM, Gopalan PK, Link DC. CXCR2 and CXCR4 antagonistically regulate neutrophil trafficking from murine bone marrow. J Clin Invest. 2010;120(7):2423-2431.
10. Baggiolini M. Chemokines in pathology and medicine. J Intern Med. 2001;250(2):91-104.
11. The human protein atlas: CXCR2 - single cell types. Available from v24.0 proteinatlas.org. URL: https://www.proteinatlas.org/ENSG00000180871-CXCR2/single+cell+type. [Accessed on 2025, Mar 22]
12. Karlsson M, Zhang C, Méar L, et al. A single–cell type transcriptomics map of human tissues. Sci Adv. 2021;7(31):eabh2169.
13. Richards S, Aziz N, Bale S, et al. Standards and guidelines for the interpretation of sequence variants: a joint consensus recommendation of the American College of Medical Genetics and Genomics and the Association for Molecular Pathology. Genet Med. 2015;17(5):405-424.
14. Liu K, Wu L, Yuan S, et al. Structural basis of CXC chemokine receptor 2 activation and signalling. Nature. 2020;585(7823):135-140.
15. Mehta HM, Malandra M, Corey SJ. G-CSF and GM-CSF in Neutropenia. J Immunol. 2015;195(4):1341-1349.
16. McDermott DH, Pastrana DV, Calvo KR, et al. Plerixafor for the Treatment of WHIM Syndrome. N Engl J Med. 2019;380(2):163-170.
17. Dale DC, Firkin F, Bolyard AA, et al. Results of a phase 2 trial of an oral CXCR4 antagonist, mavorixafor, for treatment of WHIM syndrome. Blood. 2020;136(26):2994-3003.

Figure legends

Figure 1. Identification of a Norwegian family with CXCR2 deficiency in two brothers due to homozygosity for a novel CXCR2 variant. **(A)** Blood neutrophil counts for P1 in the period from 2023-2025. **(B)** Photomicrographs from bone marrow trephine biopsy of P2 taken at age 16. Top panel: 25x magnification showing hypercellular marrow with no fat cells present. Middle panel: 100x magnification showing small scattered erythroid islands (arrows) and few megakaryocytes (arrowheads) while right-shifted myelopoiesis predominates. Bottom panel: 400x magnification demonstrating numerous hypersegmented granulocytes with conspicuous thin strands of chromatin connecting nuclear lobes (arrows). **(C)** Summary of genetic information and in silico predictions for the identified *CXCR2* c.865C>T variant (p.R289C). The CXCR2 R289C variant was identified through whole exome sequencing (WES) analysis performed on genomic DNA extracted from EDTA blood samples of the patients using a QIAsymphony instrument with corresponding DNA purification kits (Qiagen). The combined annotation dependent depletion (CADD) score and allele frequency for CXCR2 were found on gnomAD v4.1.0, variant 2-218135666-C-T (GRCh38). The results from a genome wide SNP array showed that P1 had a small region of homozygosity (ROH) surrounding the CXCR2 locus on chromosome 2q35, confirming true homozygosity for the c.865C>T variant and ruling out a large deletion**. (D)** Family pedigree. **(E)** PopViz plot for known homozygous variants reported for *CXCR2* in gnomAD v4.1.0, in this publication, or in the literature(6, 7). To ensure that all registered variants were included, we selected predicted loss-of-function (LOF) and missense/in frame indel variants for CXCR2 in gnomAD v4.1.0. **(F)** Structural representation of CXCR2 in complex with monomeric IL-8, created using the cryoelectron microscopy-solved protein structure (pdb ID: 6LFO)(14) and PyMol™ v2.2.2 (Schrödinger). Left: overview with CXCR2 in cyan, IL-8 in deep purple, and amino acid Arg289 position indicated in red. Upper right: close-up view of Arg289 showing hydrogen bonds to Glu4 and polypeptide backbone of IL-8. Lower right: close-up view of Cys289.

Figure 2. The patient *CXCR2* variant causes loss of CXCR2 surface expression and signaling. HeLa cells were transfected with pcDNA3.1 vectors encoding either CXCR2 WT, CXCR2 R289C variant, or empty vector as negative control. **(A,B)** CXCR2 expression three days post transfection analyzed in whole-cell lysates using immunoblotting (A) and on the cell surface using flow cytometry (B). To visualize CXCR2 protein, cell lysates were treated with PNGaseF to remove N-linked glycosylation. **(C,D)** Two days post transfection, HeLa cells were stimulated with IL-8 (100 ng/ml) for 2 min. Phosphorylated Erk1/2 relative to total Erk1/2 was analyzed by immunoblotting from whole-cell lysates. Shown are one representative blot (C) and quantification of three replicates in two independent experiments (D), represented as fold increase of mock-treated samples (medium only). **(E,F)** 24 h post transfection, HeLa cells were treated with 2 µM proteasome inhibitor MG132 or DMSO as vehicle control for 20 h before immunoblot analysis of CXCR2 protein and GAPDH as control. (E) Immunoblots. Lysates were treated with PNGase F before loading. (F) Quantification of E and two replicate experiments. Shown are fold increase of mock-treated samples (only medium). **(G-H)** Two days post transfection, HeLa cells were immunostained and analyzed by using a LSM800 confocal microscope. Shown are immunofluorescence images of transfected HeLa cells stained for CXCR2 (green), DNA (DAPI, blue), and ER (PDI, magenta) (G) or Golgi (golgin97, magenta) (H), The scale bar (white) indicates 10 µm. **(I,J)** Colocalization of CXCR2 with ER (I) or Golgi (J), quantified with Pearson's correlation coefficients. Data are representative of two (C,D,G,I) or three (A,B,F,H,J) independent experiments. Graphs show individual values plus mean±SD. *p<0.05, ***p<0.001, ****p<0.0001, ns = not significant, unpaired two-tailed t-test (B,I,J) and paired two-tailed t-test with Holm- Šídák multiple comparisons (D,F). ns = not significant.

Figure 3. Patient peripheral blood mononuclear cells have impaired CXCR2 surface expression and chemotaxis and gene editing by CRISPR/Cas9-based homology-directed repair restores CXCR2 surface expression. (A,B) Determination of P1 *CXCR2* mRNA transcripts relative to *TBP* by RT-qPCR (A, n=3 healthy

controls) or P1 CXCR2 protein expression relative to GAPDH by immunoblotting (B). **(C)** Quantification of B and four additional replicates (n=7 healthy controls). **(D,E)** Histograms of CXCR2 protein surface expression analyzed by flow cytometry on live cells, NK cells ($CD3^{-}CD19^{-}CD56^{+}$), and monocytes ($CD14^{+}$) from peripheral blood mononuclear cells (PBMCs) from P1 and controls (n=3), quantified in E. **(F, G)** Histogram of CXCR2 protein surface expression on neutrophils ($CD45^{+}CD14^{lo}CD16^{hi}$) from whole blood from P1 and controls (n=3), quantified in G. **(H)** Migration of neutrophils from whole blood towards an IL-8 gradient in a Boyden-chamber, using 6 mm trans-well chambers with 3 µm pore membranes. The chemotactic index was calculated as fold increase in the number of cells migrating to IL-8 compared to the number of cells migrating to medium alone. **(I)** T cells were expanded from PBMCs using anti-CD3/anti-CD28 activation beads three days before gene editing. Cas9 ribonucleoprotein (RNP) complexes were assembled by incubating recombinant Cas9 protein and single guide RNA at a molar ratio of 1:2.5 at 25°C for 15 min. T cells were combined with the resulting CRISPR/Cas9 RNP, ssODN DNA template for HDR, and AZD7648 HDR enhancer, and nucleofected for CXCR2 editing. On day 10, T cells were reactivated. On day 13, *CXCR2* transcription was induced using CRISPRa. **(J)** Gene editing efficiency of *CXCR2* in PBMCs from P1. Data show the median of three technical triplicates for one donor per group. **(K, L)** CXCR2 expression on gene-edited patient PBMCs compared to unedited patient and healthy control PBMCs, analyzed on day 14, with quantification in (L). Shown are individual values plus mean ± SD. Data are representative of one (I-K), two (D-H), three (A) or five (B-C) independent experiments. Each healthy control is shown in a distinct color. *p<0.05, **p<0.01, ***p<0.001,*****p<0.0001, ns = not significant, unpaired two-tailed t-test with Welch's correction (A,C,E,G,H) or one-way ANOVA with Šídák's multiple comparisons test (L). Gating strategies for D-H and K are shown in Supplementary Figure 2C-E.

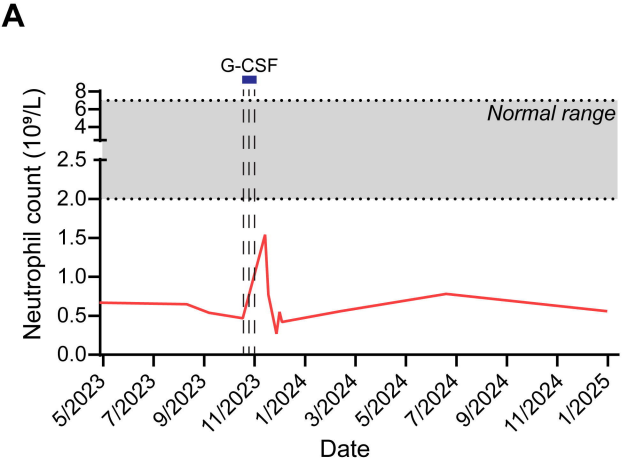

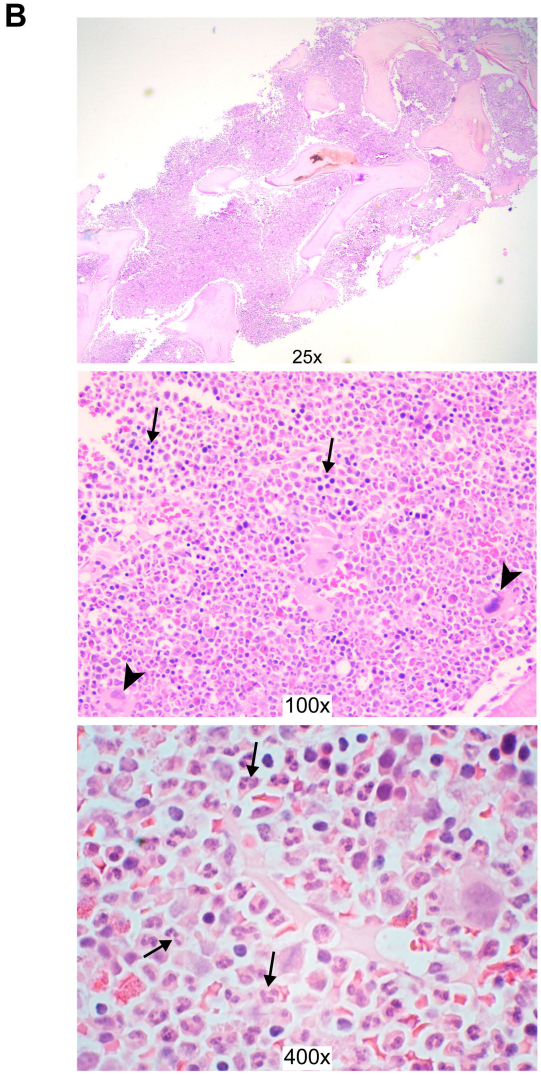

C

Genetic information	Score
Gene symbol	*CXCR2*
Transcript ID	NM_001557.4
Protein	C-X-C Motif Chemokine Receptor 2
Transcript variant	c.865C>T
Protein variant	p.R289C
Translation impact	Missense
GnomAD frequency	0.00008984
CADD (MSC 95%)	23.5 (11.2)

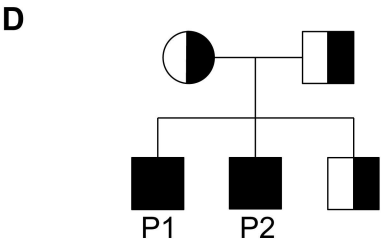

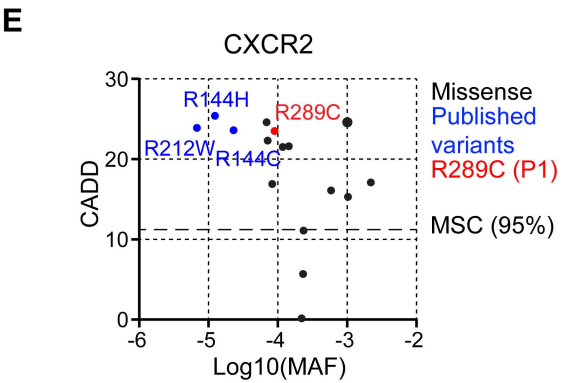

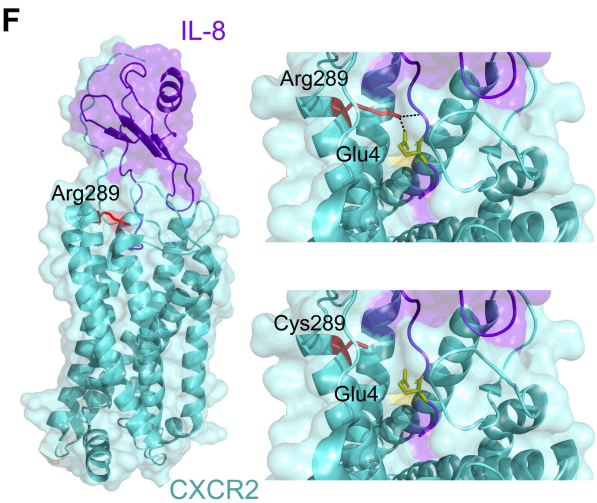

HeLa cells

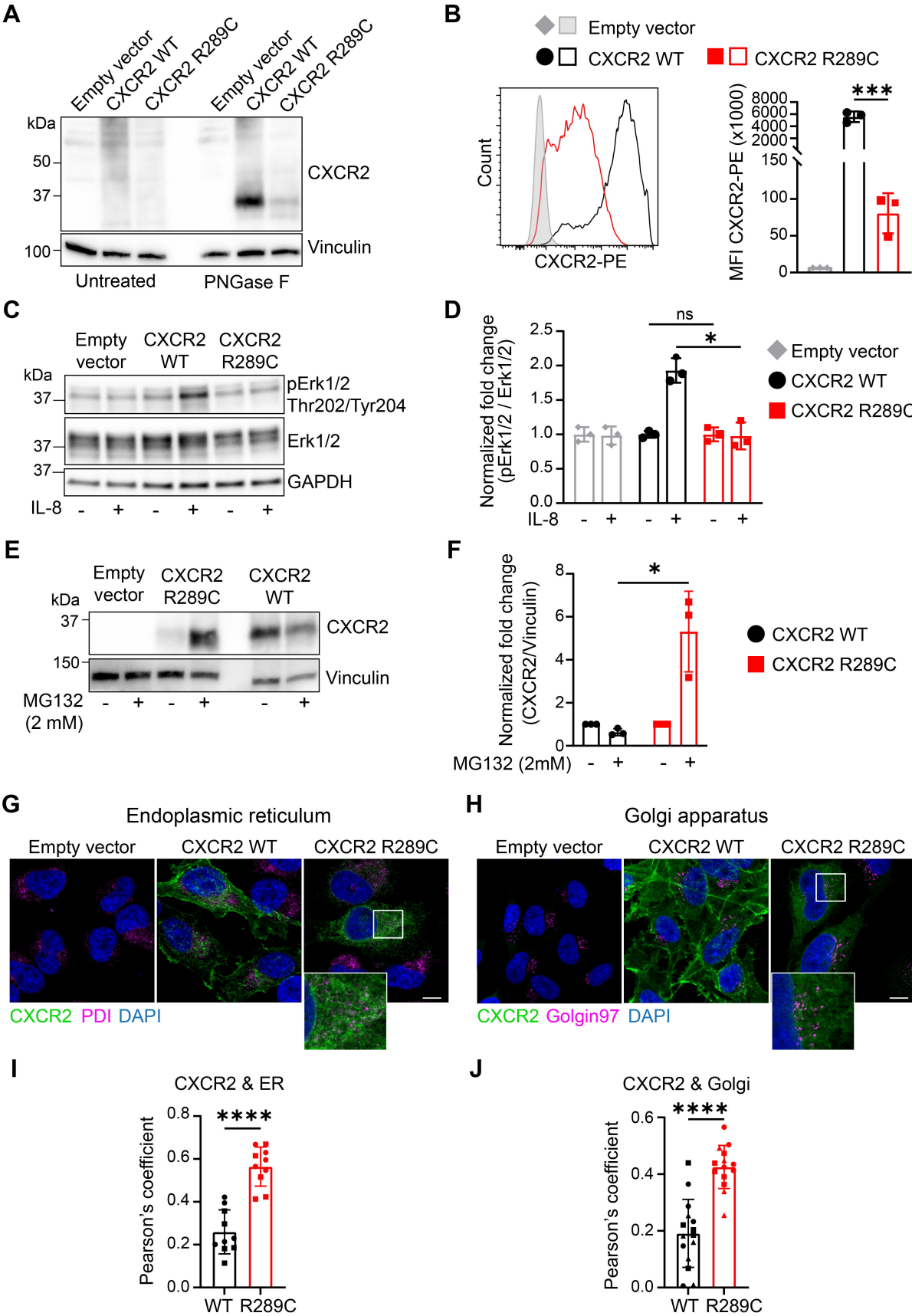
A
Empty vector
CXCR2 WT
CXCR2 R289C
Empty vector
CXCR2 WT
CXCR2 R289C
kDa
50
37
100
CXCR2
Vinculin
Untreated
PNGase F
B
Empty vector
CXCR2 WT
CXCR2 R289C
Count
CXCR2-PE
***
MFI CXCR2-PE (x1000)
8000
6000
4000
2000
150
100
50
0
C
Empty vector
CXCR2 WT
CXCR2 R289C
kDa
37
37
37
pErk1/2 Thr202/Tyr204
Erk1/2
GAPDH
IL-8 - + - + - +
D
Normalized fold change (pErk1/2 / Erk1/2)
ns
*
2.5
2.0
1.5
1.0
0.5
0.0
IL-8 - + - + - +
Empty vector
CXCR2 WT
CXCR2 R289C
E
Empty vector
CXCR2 R289C
CXCR2 WT
kDa
37
150
CXCR2
Vinculin
MG132 (2 mM) - + - + - +
F
Normalized fold change (CXCR2/Vinculin)
*
8
6
4
2
0
MG132 (2mM) - + - +
CXCR2 WT
CXCR2 R289C
G
Endoplasmic reticulum
Empty vector
CXCR2 WT
CXCR2 R289C
CXCR2 PDI DAPI
H
Golgi apparatus
Empty vector
CXCR2 WT
CXCR2 R289C
CXCR2 Golgin97 DAPI
I
CXCR2 & ER
Pearson's coefficient
****
0.8
0.6
0.4
0.2
0.0
WT R289C
J
CXCR2 & Golgi
Pearson's coefficient
****
0.6
0.4
0.2
0.0
WT R289C

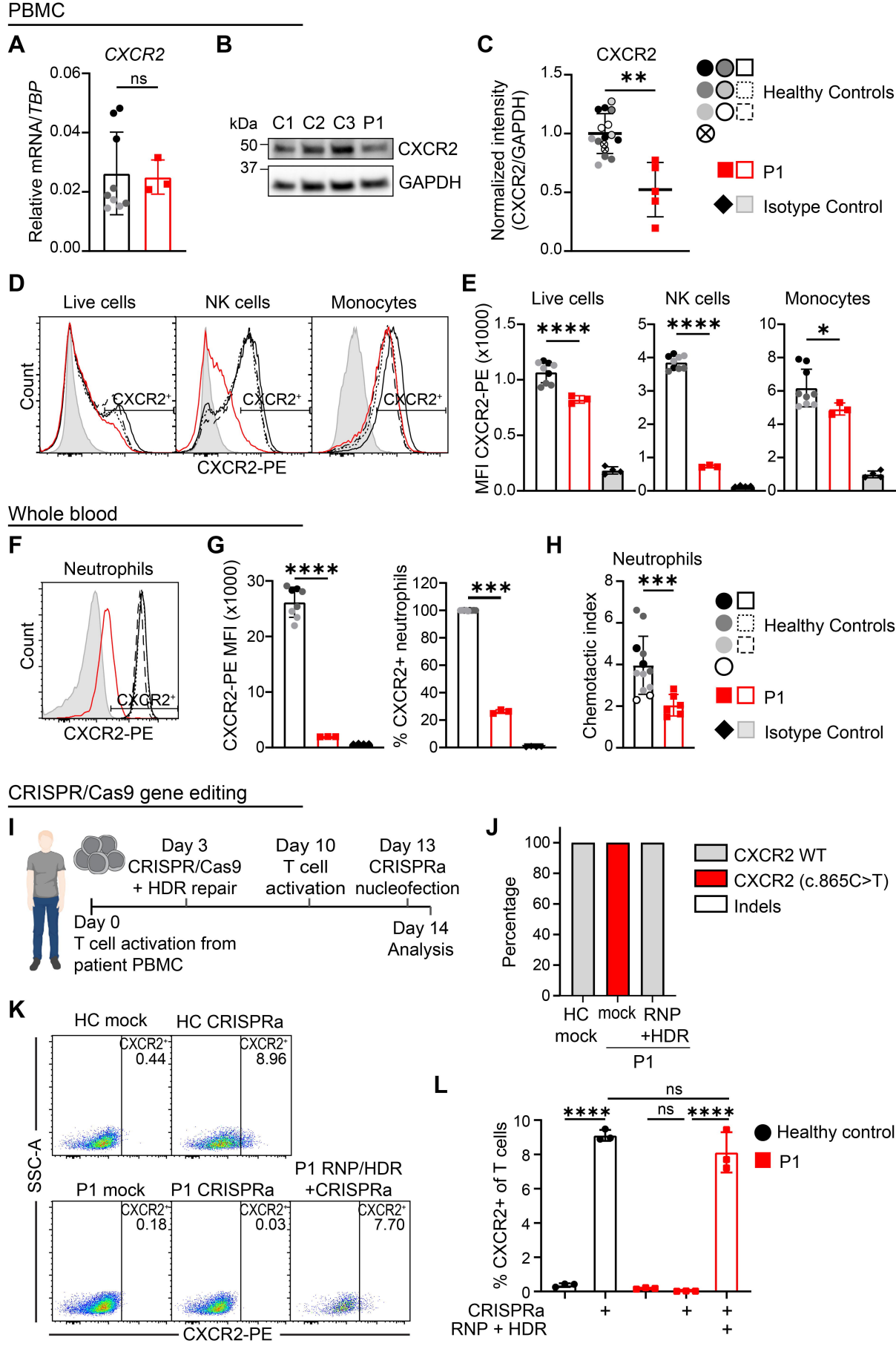
PBMC
A
CXCR2
ns
Relative mRNA/TBP
0.06
0.04
0.02
0.00
B
kDa C1 C2 C3 P1
50
37
CXCR2
GAPDH
C
CXCR2
**
Normalized intensity (CXCR2/GAPDH)
1.5
1.0
0.5
0.0
Healthy Controls
P1
Isotype Control
D
Live cells
NK cells
Monocytes
Count
CXCR2+
CXCR2-PE
E
Live cells
NK cells
Monocytes
MFI CXCR2-PE (x1000)
****
****
*
Whole blood
F
Neutrophils
Count
CXCR2+
CXCR2-PE
G
CXCR2-PE MFI (x1000)
****
% CXCR2+ neutrophils
***
H
Neutrophils
Chemotactic index
***
Healthy Controls
P1
Isotype Control
CRISPR/Cas9 gene editing
I
Day 3
CRISPR/Cas9
+ HDR repair
Day 10
T cell
activation
Day 13
CRISPRa
nucleofection
Day 0
T cell activation from
patient PBMC
Day 14
Analysis
J
Percentage
100
80
60
40
20
0
CXCR2 WT
CXCR2 (c.865C>T)
Indels
HC mock
mock
RNP
+HDR
P1
K
HC mock
HC CRISPRa
CXCR2+
0.44
CXCR2+
8.96
P1 mock
P1 CRISPRa
P1 RNP/HDR
+CRISPRa
CXCR2+
0.18
CXCR2+
0.03
CXCR2+
7.70
SSC-A
CXCR2-PE
L
ns
****
ns
****
% CXCR2+ of T cells
Healthy control
P1
CRISPRa
RNP + HDR

Supplementary information for

CXCR2 deficiency with myelokathexis caused by a novel variant: correction via CRISPR/Cas9

Daniëla M. Hinke[1,2,3], Sofie R. Dorset[1], Eirik Bratland[4], Jonas H. Wolff[1,3], Astrid M. Olsnes[5,6], Jacob Giehm Mikkelsen[1,3], Lars Hegeland[7], Rasmus O. Bak[1], Andreas Benneche[4], and Trine H. Mogensen[1,2,3]*

1. Department of Biomedicine, Aarhus University, Aarhus, Denmark

2. Department of Infectious Diseases, Aarhus University Hospital, Aarhus, Denmark

3. Center for Immunology of Viral infections (CIVIA), Aarhus University, Aarhus, Denmark

4. Department of Medical Genetics, Haukeland University Hospital, Bergen, Norway

5. Department of Clinical Science, University of Bergen, Norway

6. Section for Hematology, Department of medicine, Haukeland University Hospital, Bergen, Norway

7. Section for Pathology, Haukeland University Hospital, Bergen, Norway

*Correspondence: Trine H Mogensen, Department of Biomedicine, Aarhus University, Wilhelm Meyers Allé 4, 8000 Aarhus C, Denmark; mail trine.mogensen@biomed.au.dk

This document contains

Supplementary table 1

Supplementary figures 1-2

Supplementary Table 1. Comparison of genetic characteristics of *CXCR2* variants and clinical presentation of patients from different publications, including the patients described in this paper (P1 and P2) and patients from Auer et al.[5], Marin-Esteban et al.[6], and Klimiankou et al.[7].

Publication, pt	Hinke et al., P1	Hinke et al., P2	Marin-Esteban et al., P1[6]	Marin-Esteban et al., P2[6]	Marin-Esteban et al., P3[6]	Marin-Esteban et al., P4[6]	Auer et al., P1[5]	Auer et al.,P2[5]	Klimiankou et al., P1[7]	Klimiankou et al., P2[7]	Klimiankou et al., P3[7]
Sex	M	M	F	F	F	M	F	F	F	F	F
Variant in *CXCR2*	c.865C>T (p.R289C)	c.865C>T (p.R289C)	CXCR2 del	c.430C>T, p.R144C	c.634C>T, pR212W	c.550C>T/c 865C>T (p.R184*/p .R289C)	c.986delA (p.H323fs6*)	c.986delA (p.H323fs6*)	c.431G>A, p.(R144H)	c.431G>A/c.720_727del p.(R144H)/p.(Lys240AsnfsTer45)	c.431G>A/WT p.(R144H)/ WT
GnomAD frequency	0.00008984	0.00008984	NA	0.00002292	0.000006814	NA	NA	NA	0.0000124	0.0000124/ NA	0.0000124
CADD score	23.5‡	23.5‡	NA	31§	23.1§	23§	NA	NA	25.4‡	25.4‡	25.4‡
Baseline neutrophil levels (x 10^9/L)	0.5-1.2†	0.1-0.4	0.28-1.8	0.1-0.85	0.1-10.8†	0.3-1	0.1 – 0.2	0.5-1.2	0.3	0.5	1.2
Other abnormal lab value?	Elevated IgG and IgA	Elevated IgG	Elevated IgG and IgM	Elevated IgG	Elevated IgM	Elevated B cells and NK cells	NA	NA	Anti-Fcg-RIIIb auto-antibodies	No	No
Myeloka-thexis	Yes	Yes (33%)	Yes (35%)	No	No	No	Yes	Yes	No	No	No
Clinical manifesta-tions	Oral ulcerations recurrent upper respiratory tract infections	Ulcerations lips, oral cavity, and nose	Oral lesions	Oral lesions, cellulitis episode	Oral lesions, pneumoni-tis episode	Oral lesions	Recurrent bacterial infections, septic thrombo-phlebitis, subacute bacterial endocarditis	Few infectious episodes	Frequent upper airway- and skin infections	Recurrent pharyngitis, bronchitis, and oral ulcerations	No history of recurrent infections

†Neutrophil counts increased spontaneously during infectious episodes. ‡ CADD score from gnomAD v4.1.0 database. § CADD score reported by in publication; NA = information not available

A

Characteristic	Normal range	Values P1	Values P2
Clinical profile			
Age at diagnosis (years)		3	16
Oral lesions		Yes	Yes
Infections		Yes	Yes, mild
G-CSF therapy (dose, period)		Yes (15 MU and 30 MU, 3 weeks)	Yes (48 MU, one administration)
Age at last follow-up (years)		29	23
CRP	<8.0	<4.0	4
Hematologic values			
Total leukocytes (10^9/L)	3.5 - 10.0	2.8	1.8
Neutrophils (10^9/L)	1.8 - 6.9	0.78	0.1
Monocytes (10^9/L)	0.20 - 0.70	0.54	0.38
Lymphocytes (10^9/L)	1.30 - 3.50	1.28	1.1
Basophils (10^9/L)	<0.1	0.04	0
Platelets (10^9/L)	145 - 350	305	376
Hemoglobin (mmol/L)	8.3 - 10.5	8.8	13.6
Immunoglobulin levels			
IgA (g/L)	0.80 - 3.90	4.96	
IgG (g/L)	6.1 - 14.9	17.1	
IgM (g/L)	0.39 - 2.08	0.80	

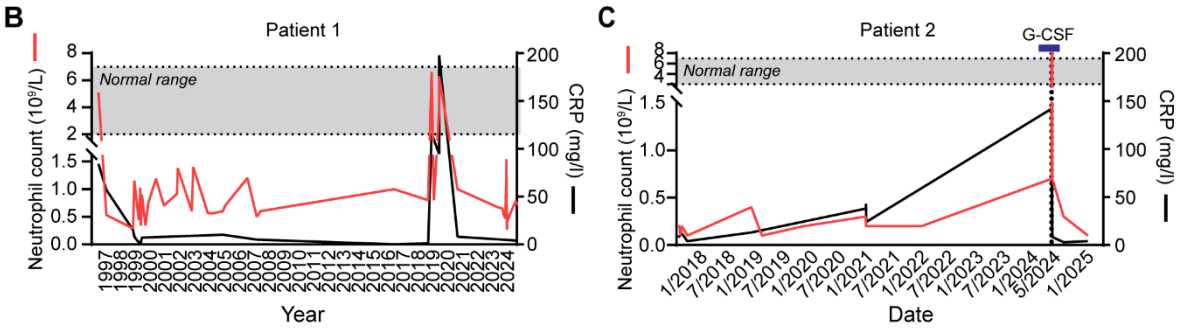

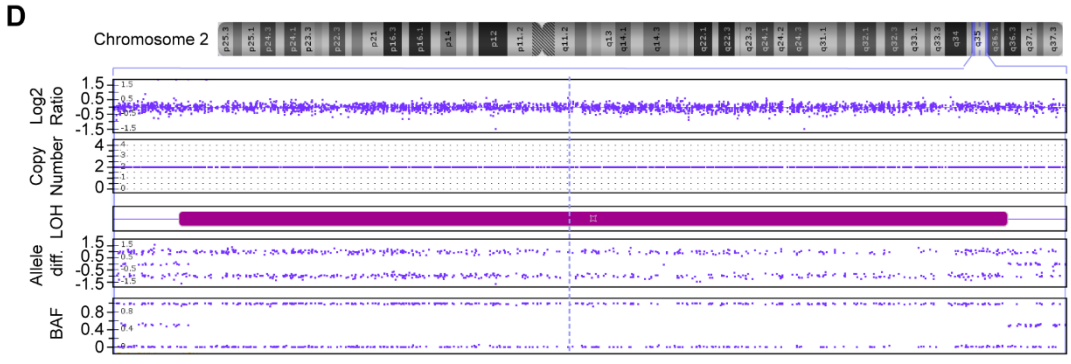

E

Classification of CXCR2 R289C variant according to ACMG/AMP

Supporting	
PP1	Cosegregation with neutropenia in two families represented herein and in ref. 6
PP2	Low allele frequency of <0.01
PP3	Various computational algorithms support a deleterious effect (CADD>MSC, SIFT 0.01, PolyPhen2 1.0)
Moderate	
PM3	The variant was reported in trans with pathogenic variant p.Arg184Ter in ref. 6
Strong	
PS3	Functional studies herein and in ref. 6 support a damaging effect of the variant on the gene product

Sum: 1 strong + 1 moderate + 3 supporting criteria → Classifies R289C variant as likely pathogenic

Supplementary Figure 1. Clinical blood values and neutrophil count for P1 and P2 plus SNP array and pathogenic evaluation of patient variant. (A) Clinical and immunological blood values for P1 and P2

during the last follow-up visits. Red indicates that the value is lower, and underlined indicates that the value is higher than the normal range (defined by Danish medical standard). **(B)** Extended blood neutrophil levels and CRP for P1 in the period from 1996-2025. **(C)** Blood neutrophil levels and CRP for P2 in the period from 2017-2025. Date for G-CSF treatment is indicated. Abbreviations: G-CSF: granulocyte colony-stimulating factor; CRP: C-reactive protein; MU: million units. **(D)** Results of a genome wide SNP array. Emphasized is a 3.3 kb region of a long continuous stretch of homozygosity encompassing the CXCR2 locus in chromosome 2q35: arr[GRCh37] 2q35(217451281_220734778). The CXCR2 locus is marked in the figure by an interrupted blue line. LOH: Loss of heterozygosity. Allele diff: Allele difference; BAF: B-allele frequency. **(E)** The CXCR2 R289C variant was classified as likely pathogenic according to guidelines from the American college of Medical Genetics (ACMG)/ Genomics and Association for Molecular Pathology (AMP)[13] supplemented with recommendations from ClinGen (https://www.clinicalgenome.org/working-groups/sequence-variant-interpretation) and the UK Association for Clinical Genomic Science (ACGS) (https://www.acgs.uk.com/media/12533/uk-practice-guidelines-for-variant-classification-v12-2024.pdf).

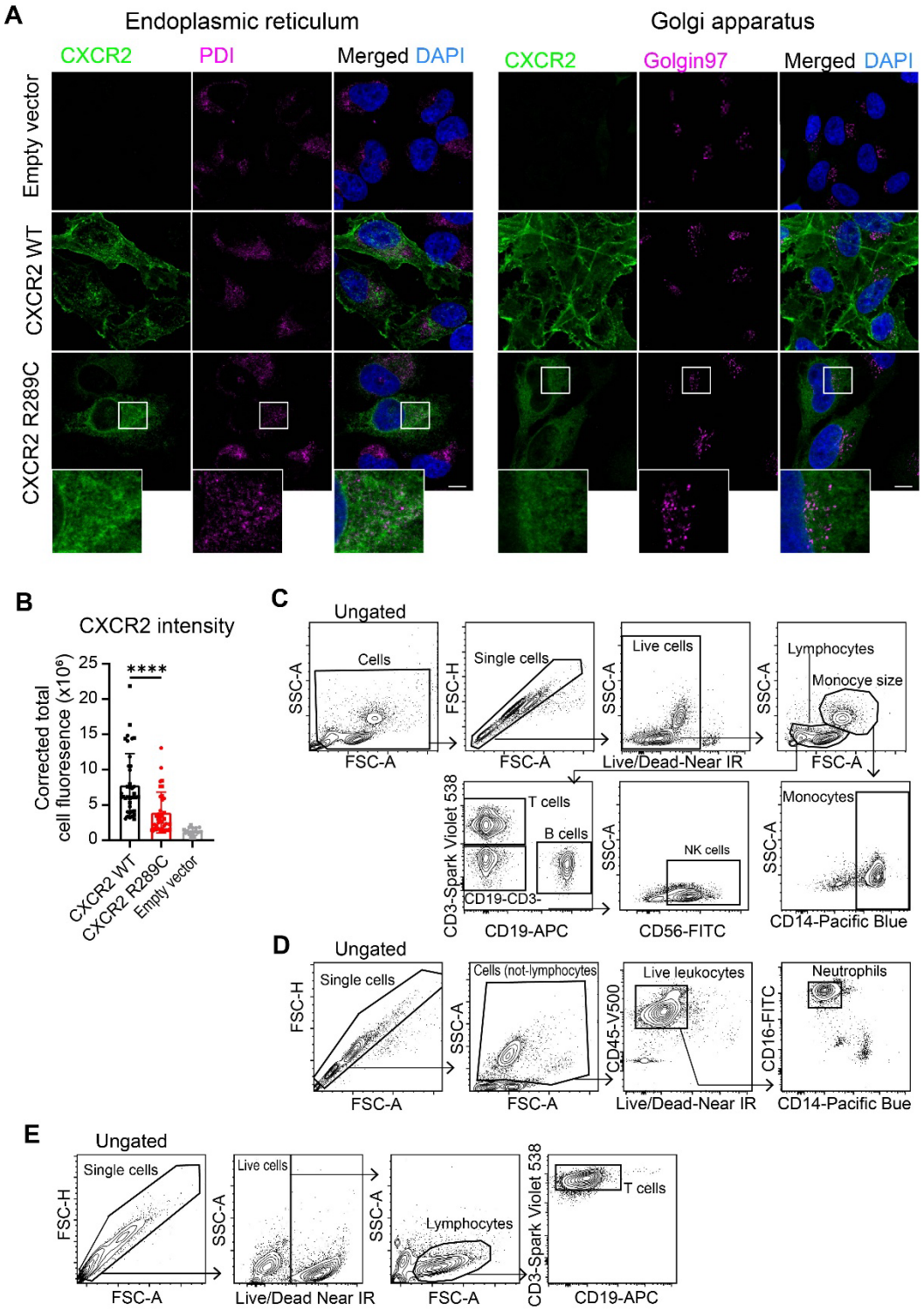

Supplementary Figure 2. Confocal and flow cytometry data. (A-B) HeLa cells were transfected with pcDNA3.1 vectors encoding either CXCR2 WT, CXCR2 R289C variant, or empty vector as negative control. Two days post transfection, cells were stained for CXCR2 (green), DNA (DAPI, blue), and ER (PDI, magenta) or Golgi (golgin97, magenta). (A) Immunofluorescence images. The scale bar (white) indicates 10 µm. (B) Quantification of the corrected cell fluorescence of CXCR2. Two experiments are

shown. Values for each experiment are shown with different symbols. Shown are individual values plus mean ±SD. **** p<0.0001, unpaired two-tailed t-test. **(C)** Gating strategy for Figure 3D for identification of live monocytes ($CD14^+$), B cells ($CD19^+CD3^-$), T cells ($CD19^-CD3^+$) and NK cells ($CD19^-CD3^-CD56^+$) from PBMCs. **(D)** Gating strategy for Figure 3F-H for identification of live neutrophils ($CD45^+CD14^{lo}CD16^{hi}$) from whole blood for analysis of CXCR2 expression and neutrophil migration in chemotaxis assay. **(E)** T cells were expanded from PBMCs using anti-CD3/anti-CD28 activation beads three days before editing with CRISPR/Cas9 RNP, ssODN DNA template for HDR, and AZD7648 HDR enhancer. On day 10, T cells were treated with expansion beads a second time. On day 13, CXCR2 transcription was induced using CRISPRa. CXCR2 surface expression on T cells was analyzed on day 14. Shown here is the gating strategy for the identification of T cells ($CD3^+CD19^-$) for Figure 3K-L.